

Dynamic Behavior of Transport in Normal and Reversed Shear Plasmas with Internal Barriers in JT-60U

S. V. Neudatchin 1,2), T. Takizuka 2), Yu. N. Dnestrovskij 1), H. Shirai 2), T. Fujita 2),
A. Isayama 2), Y. Kamada 2), Y. Koide 2)

1) Nuclear Fusion Institute, RRC "Kurchatov Institute", Moscow, Russia
2) Japan Atomic Energy Research Institute, Naka Fusion Research Establishment
Naka-machi, Naka-gun, Ibaraki-ken 311-0193, Japan

e-mail contact: neudatsv@fusion.naka.jaeri.go.jp

Abstract. Transport evolution in reverse shear (RS) and normal shear (NrS) JT-60U tokamak plasmas with internal transport barrier (ITB) is described as a combination of various fast and slow time scales processes. Abrupt in time and wide in space (~ 0.3 of minor radius) variations of electron and ion heat diffusivities $\delta\chi_{e,i}$ (seen as "spontaneous-like" simultaneous rise and decay of $T_{e,i}$ in two spatial zones) are found for weak ITBs in both RS and NrS plasmas. Profiles of $\delta\chi_{e,i}$ in RS plasmas with strong ITB are usually localized near ITB "foot" inside smaller space region. The maximum of the heat flux variation is located near position of the minimum of safety factor q in various RS plasmas, and variation is extended in positive shear region. Inward and outward heat pulse propagations created by $\delta\chi_{e,i}$ and sawtooth-like crashes are analyzed, small values of $\chi_{e,i}$ and absence of "heat pinch" are found in ITB region. Another source of abrupt $\delta\chi_{e,i}$ inside most of plasma volume, including significant part of weak ITB in RS plasmas, is seen as ELM-induced H-L transitions.

1. Introduction

Significant progress is seen in the development of the Steady State RS (SSRS) scenario [1] and Steady State high- β_p scenario with Normal Shear (NrS) [2] in JT-60U plasmas with ITB. Understanding the ITB properties and finding the control method of the ITB are among the mostly important issues for the tokamak fusion research. Processes of the transport evolution during RS and NrS discharges have not been fully understood yet. Abrupt variations of ITB properties in RS JT-60U plasmas were reported in [3] and studied in more detail recently [4]. Abrupt in time (within a few ms) and spatially wide variations of $\chi_{e,i}$ ($\delta\chi_{e,i}$) were found in [4]. Such phenomena, with "bipolar" perturbation of $T_{e,i}$ ($T_{e,i}$ rise in one zone simultaneous with decay of $T_{e,i}$ in another zone) are called here "ITB-events". Abrupt variations of χ_e were found earlier in NrS plasmas with ITB [5], but profiles of $\delta\chi_e$ were not obtained. Two types of ITB with various transport properties, "parabolic" (or weak) and "box-type" (or strong), were observed in JT-60U RS plasmas [6]. The 12-channel high-space-resolution ECE heterodyne radiometer was used for T_e measurements (channel 1 is called below ch. 1, etc.)

2. ITB-events in NrS and RS plasmas

In this section, we first analyze ITB evolution in NrS 1.5MA/3.8T discharge E34487. Waveforms of this NBI-heated discharge are shown in Fig. 1(a) with: the injected NB power P_{NB} ; the stored energy measured with diamagnetic loop, W_{dia} ; the ion and electron temperatures, $T_{e,i}$, measured near $\rho = 0.4$ for ions and near $\rho = 0.4, 0.65$ for electrons, where ρ denotes the volume averaged minor radius normalized by the radius of a separatrix magnetic surface. We can briefly describe the plasma evolution shown in Fig. 1(a) as follows. Weak ITB is created before 4.6s as clearly observed on the T_i profile (circles) in Fig. 1(b). ITB-event is occurred at $t=4.602s$ shown by the vertical line in Fig 1(a). The rise of $T_i(0.4)$ and "bipolar" perturbation of T_e (rise of $T_e(0.4)$ and decay of $T_e(0.65)$) are clearly observed in Fig. 1(a) and highlighted by arrows with (+) and (-) signs. Positions of radiometer channels 1 and 12 are shown in Fig. 1 by vertical dashed lines. After ITB-event, abrupt rise of T_e is observed at ch. 1-7, and decay at ch. 10-12. Profiles of T_{ie} 90 ms after ITB-event are shown in Fig. 1(b) by solid lines. ITBs are either improved by ITB-events (negative $\delta\chi_e$) or degraded by them (positive $\delta\chi_e$). We may call this ITB-event ITB "improvement" or, at the same time, "formation" of strong ITB from weak one. The negative profile of $\delta\chi_e$ (obtained from abrupt variation of dT_e/dt values like those described in [4]) are shown in Fig. 1(c) by circles. The negative profile of $\delta\chi_e$ obtained for ITB-event in RS pulse 32423 with weak ITB (see Fig. 5 in [4]) is shown by squares in Fig. 1(c). Space positions of channels 1-12 are taken from 0.37 to 0.66 of minor radius in RS and from 0.29 to 0.67 in NrS plasmas. Profiles of $\delta\chi_e$ are similarly

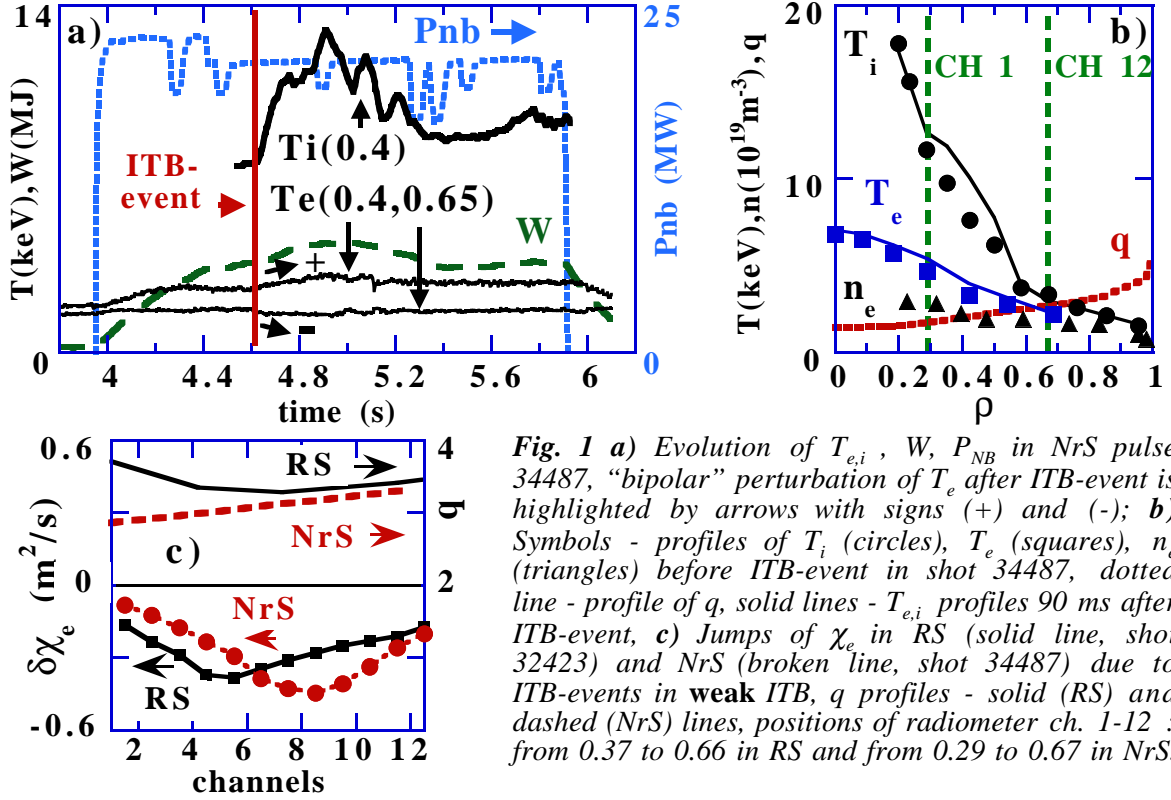


Fig. 1 a) Evolution of $T_{e,i}$, W , P_{NB} in NrS pulse 34487, “bipolar” perturbation of T_e after ITB-event is highlighted by arrows with signs (+) and (-); b) Symbols - profiles of T_i (circles), T_e (squares), n_e (triangles) before ITB-event in shot 34487, dotted line - profile of q , solid lines - $T_{e,i}$ profiles 90 ms after ITB-event, c) Jumps of χ_e in RS (solid line, shot 32423) and NrS (broken line, shot 34487) due to ITB-events in weak ITB, q profiles - solid (RS) and dashed (NrS) lines, positions of radiometer ch. 1-12 : from 0.37 to 0.66 in RS and from 0.29 to 0.67 in NrS.

wide for both ITB-events in NrS and RS plasmas with weak ITBs while MSE-measured q profiles shown in Fig 1(c) are totally different. T_e profiles just before and 15ms after ITB-event in RS plasmas (1.5MA/3.8T shot E32424) with strong ITB are shown in Fig 2a by solid and dashed curves, respectively. ITB-event “improvement” is seen as T_e rise in small region (initially on ch. 7 and 8 as marked in Fig 2(a)) and decay on ch.11, 12. Profile of $\delta\chi_e$ shown in Fig. 2(a) (dotted curve, calculated as in [4]) is localized near ITB “foot”, compared with spatially wider $\delta\chi_e$ profiles in weak ITB case, and extended to positive shear region (at least slightly outside ch.12, well above error bars). Value of $\delta\chi_e$ is inversely proportional to ∇T_e while ∇T_e is not well-known in the region outside q_{min} , with small values of ∇T_e . Gradual diffusive broadening of rising positive T_e perturbation δT_e is observed later in time and is analyzed in Section 3 below.

3. Inward and Outward Heat Pulse Propagation inside ITB in RS.

The new source of heat pulse propagation (HPP) - ITB-event induced inward HPP is found and indicated by the arrow in Fig. 2(a). The evolution of T_e (ch.6, 5) is shown in Fig. 2(b), the time of ITB-event is marked by symbol A, 15 ms later time marked by B. A few ms time delay in T_e rise is clearly observed on ch.6. Inward HPP from ch.6 to ch.5 is schematically shown by the arrow in Fig. 2(a). HPP is analyzed with numerical solution of δT_e transport equation solved in the region $0 \leq r \leq r_6$ with zero initial condition, the right boundary condition $\delta T_{e,CAL}(r_6,t) = \delta T_{e,EXP}(r_6,t)$ being taken from experiment, with left boundary condition $d\delta T_e(0,t)/dr = 0$. The value of $\chi_e^{HP} = 0.12(0.05-0.23)$ m²/s is found from the best fit of the calculated and experimental data on ch.5.

We now analyze outward HPP created by another new source observed as sawtooth-like crash in central part of RS plasmas. T_e profiles before and after the crash in 1.8MA/3.7T shot E36614 with strong ITB are shown in Fig 2c by solid and dashed curves, correspondingly. Location of ch.1 and 12 is taken equal to $r/a=0.3$ and 0.62. Timetraces of T_e (ch. 9-12) are shown in Fig. 2(d), crash-induced T_e rise is observed on ch. 9,10. Since no clear response on ch. 11 is observed, one can not obtain χ_e^{HP} value but are can estimate χ_e^{HP} upper limit only. Outward HPP is analyzed similarly to the one described above for inward HPP, but in the region between r_{10} and separatrix r_{SEP} . Left boundary condition $\delta T_{e,CAL}(r_{10},t) =$

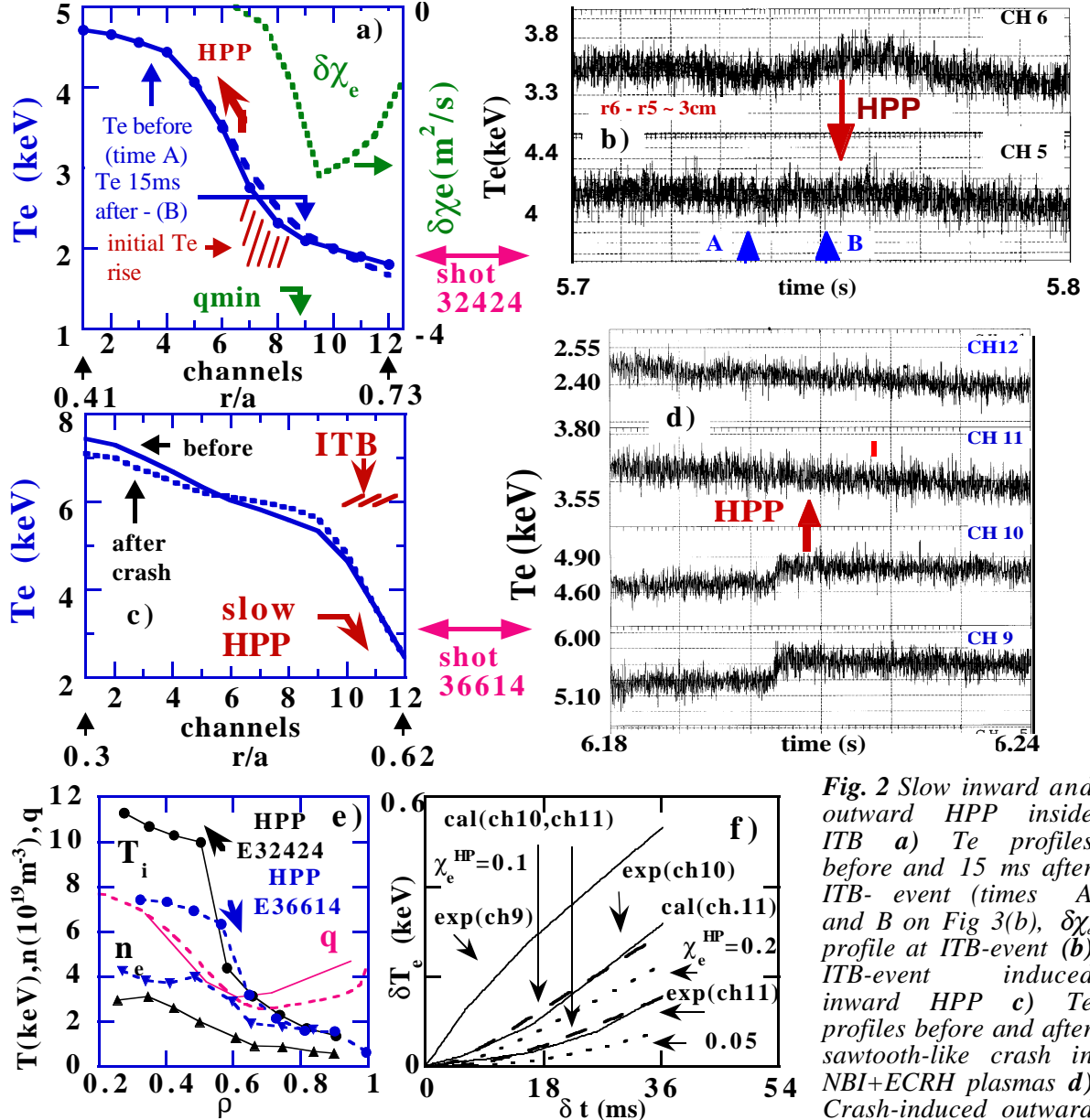


Fig. 2 Slow inward and outward HPP inside ITB a) T_e profiles before and 15 ms after ITB- event (times A and B on Fig 3(b), $\delta\chi_e$ profile at ITB-event (b) ITB-event induced inward HPP c) T_e profiles before and after sawtooth-like crash in NBI+ECRH plasmas d) Crash-induced outward

HPP from radiometer ch 10 to ch 11 e) Profiles of T_i (circles), n_e (triangles) and q before HPP in E32424 (solid lines) and E36614 (dashed lines), HPP regions are shown by arrows; f) ITB-event induced outward HPP from ch.9 to ch.10,11 inside ITB in $s>0$ region in shot E32423.

$\delta T_{e, \text{EXP}}(r_{10}, t)$ is taken from experiment, $\delta T_{e, \text{CAL}}(r_{\text{SEP}}, t) = 0$ is chosen as the right boundary condition. The magnitude of $\delta T_{e, \text{CAL}}(r_{11}, t_{\text{CRASH}} + 15 \text{ms})$ obtained with $\chi_e^{\text{HP}} = 0.1 \text{m}^2/\text{s}$ is shown in Fig. 2(d) by solid vertical gray short segment. Values of $\chi_e^{\text{HP}} < 0.06 \text{m}^2/\text{s}$ are obtained from HPP analysis. Profiles of T_i (circles), n_e (triangles) and q before HPP in shot E32424 ($P_{\text{NB}} = 10.5 \text{MW}$, $W = 2.8 \text{MJ}$, $\tau_E \sim 0.25 \text{s}$) and in shot E36614 ($P_{\text{NB}} = 5.4 \text{MW}$, $P_{\text{ECRH}} = 1.2 \text{MW}$, $W = 3.2 \text{MJ}$, $\tau_E \sim 0.5 \text{s}$) are compared in Fig 2(e). Location of electron HPP regions is shown by arrows. In shot E36614, T_i is close to T_e in the region of HPP study (due to ECRH and higher density), while $T_e \sim 0.5 T_i$ in the same region of the shot E32424 plasmas.

Formation of strong ITB in positive shear zone of RS plasmas (shot E32423) is described as series of 3 consecutive ITB-events [7]. Evolution of δT_e (induced by the third ITB-event) is observed as outward HPP from ch. 9 to ch. 10,11 (throughout ITB-event improved confinement region) is shown in Fig. 3(f) by solid (experiment), dashed lines (calculations for ch. 10,11 with $\chi_e^{\text{HP}} = 0.1 \text{m}^2/\text{s}$) and dotted lines (calculations for ch. 11 with $\chi_e^{\text{HP}} = 0.2$ and $0.05 \text{m}^2/\text{s}$). Values of χ_e^{HP} as low as $\sim 0.1 \text{m}^2/\text{s}$ are obtained from electron and ion HPP in the $\sim 8 \text{cm}$ width region fully localized in positive shear space zone of RS plasmas.

4. ITB response to ELM-induced H-L transitions in RS.

The ways to obtain L-H transition in RS JT-60U plasmas are described in [1]. Waveforms of NBI-heated 1.5MA/3.8T discharge 32419 (weak ITB phase) are shown in Fig. 3(a) with: the injected NB power P_{NB} ; the stored energy W ; $H\alpha$ signal from the divertor. Many ELMs with post-ELM enhanced $H\alpha$ level ($\sim 5\div 100$ ms duration in various pulses) are clearly observed in Fig. 3(a). We analyze plasma response to ELM labeled by arrow marked t_1 in Fig. 3(a) in detail. Profiles of T_i (circles), n_e (triangles) and q (dotted line) before $t=t_1$ are shown in Fig 3(b), location of radiometer ch.1 and 12 ($r/a=0.39$ and 0.69) is marked by vertical dashed lines. ELM-induced H-L back transition is observed on $H\alpha$ shown in Fig. 3(c). The transition is seen as abrupt and simultaneous linear decay of T_e inside ITB (ch. 1-7), shown for ch.1 in Fig. 3(d). Decay of T_e is well correlated (~ 2 ms) with abrupt rise of $H\alpha$. The same T_e behavior is observed for ELMs before $t=t_1$. T_e profiles before and 10ms after transition are shown in Fig. 3(e). The zone shown in Fig. 3(e) is located in RS region. Decrease of T_e is created by abrupt $\delta\chi_e$ shown on Fig. 3(e) by circles and calculated as reported in [4] with small correction for inward plasma motion due to energy losses (same role of plasma motion obtained just recently from T_e decay measured from low and high field side by grating polychrometer, and by radiometer from low field side in another shot). Value of $\delta\chi_e$ is inversely proportional to ∇T_e while ∇T_e is not well-known in the region outside q_{min} , with small values of $\nabla T_{e,i}$. Decay of T_e on ch. 1-6 can be explained (still with some delay and slightly less δT_e amplitude on ch. 1-3) by inward HPP from ch. 7 calculated with $\chi_e^{HP} \sim 10\text{m}^2/\text{s}$ (order of amplitude above χ_e^{PB} calculated from power balance). A significant part of weak ITB located in RS zone is covered by abrupt increase of χ_e .

Response of strong ITB to ELM-induced H-L transitions is not fully clear at present. The region of T_e decay induced by irregularly observed ELM-like phenomena (with $H\alpha$ level enhanced by $\sim 50\%$ for 5-10 ms) is limited by ITB foot and T_e decay is not penetrated inside ITB region, but in ELMs-induced L-modes $H\alpha$ level is typically enhanced by 2-3 times.

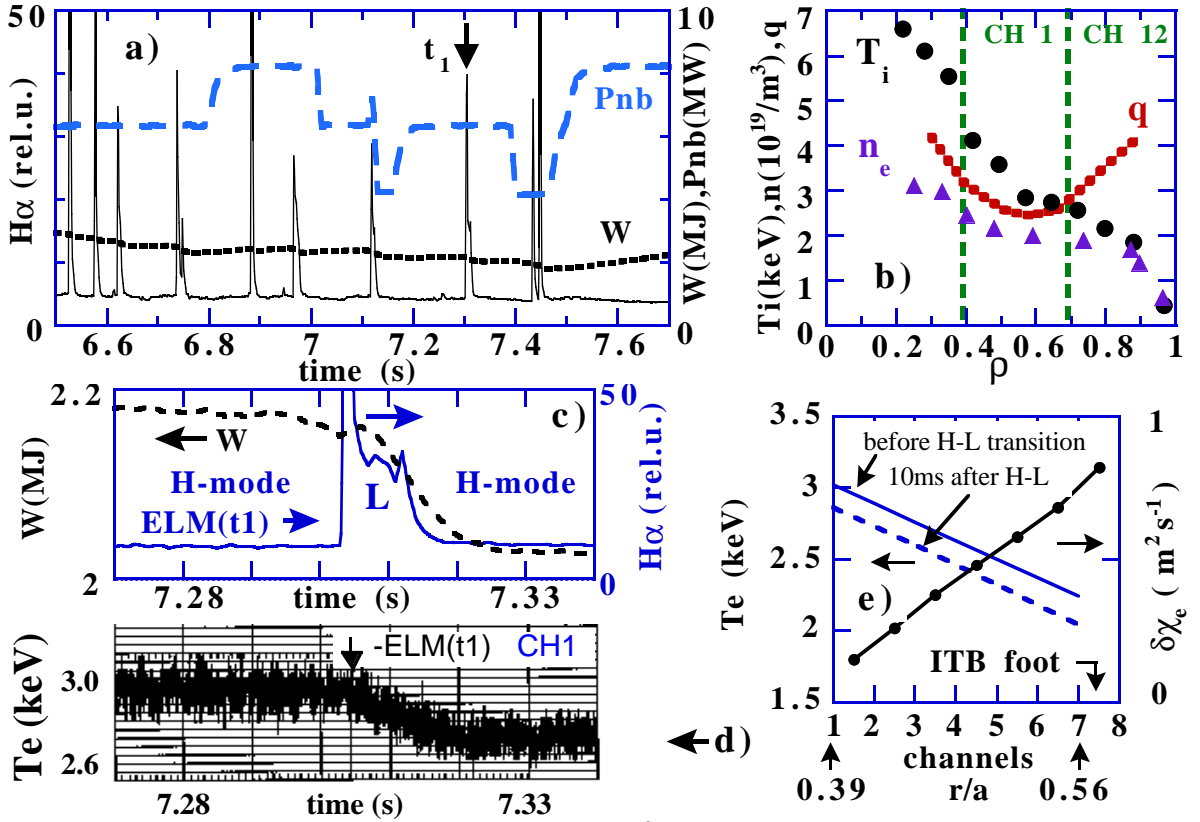


Fig. 3 ITB response to H-L in RS shot 32419 with weak ITB: a)- timetraces of $H\alpha$, W , P_{nb} ; t_1 - time of ELM shown in Figs. 3(c) and 3(d); b)- profiles of T_e , n_e , q before ELM at $t=t_1$; (c) and (d)- evolution of $H\alpha$, W , T_e (ch.1) around $t=t_1$; e)- change of T_e and χ_e at H-L transition at $t=t_1$.

5. Discussion and Conclusions

Surprisingly wide (~ 0.3 of minor radius) profiles of $\delta\chi_e$ are found at ITB-events in NrS plasmas. ITB-events widths are generally similar for weak ITBs in RS and NrS plasmas. Profiles of $\delta\chi_e$ at ITB-event in RS plasmas with strong ITB are localized near ITB “foot” in comparison with wider $\delta\chi_e$ profiles in weak ITB case. In various RS pulses studied up to now, the maximum of the heat flux abrupt variation is always located near position of q_{\min} and heat flux variation is always extended to positive shear region.

New sources of HPP are found in RS plasmas. We observe symmetric picture of slow HPP ($\chi_e^{\text{HP}} \sim 0.1\text{m}^2/\text{s}$) in 3 cases: inward ITB-event induced electron HPP ($\chi_e^{\text{HP}} \approx 0.5 \chi_{i\text{ neo}}$) and outward sawtooth-like crash induced HPP ($\chi_e^{\text{HP}} < 0.2 \chi_{i\text{ neo}}$), both propagated throughout strong ITB in RS zone; outward ITB-event induced electron and ion HPP ($\chi_e^{\text{HP}} \approx \chi_i^{\text{HP}} \approx \chi_{i\text{ neo}}$) throughout strong ITB abruptly formed by ITB-event in positive shear zone of RS plasmas (this case described in [7] in detail). Important consequence of HPP analysis is the absence of electron and ion “heat pinch” in ITB region.

However, some of the JT-60U RS discharges with ITB were described by a complicated “canonical profile” (CPTM) model [8], where L-mode confinement formed by nearly balanced large inward convective and outward diffusive heat fluxes. ITB formation was described as “forgetting” of canonical profiles under some conditions and “heat pinch” was absent inside ITB.

Fast response of T_e to ELM-induced H-L back transitions (seen as T_e decay correlated within 2ms with abrupt rise of $H\alpha$) is found well inside weak ITB in RS region, suggesting edge-core interplay across q_{\min} in ms timescale. T_e decay is interpreted as abrupt appearance of negative $\delta\chi_e$. The global nature of abrupt χ_e variations inside RS region is similar to abrupt variations of $\chi_{e,i}$ in 90% of plasma volume seen under “fast” L-H-L transitions in some JT-60U [9] and JET [10] NrS regimes without clear ITB including ELM-induced long and short (few ms) L-modes on JET (first time described in JET VH-mode plasmas [10]) and ELM-induced L-modes on JT-60U [9].

Extremely complex transport evolution inside ITB has been partially described as highly dynamic system with plenty of coupled processes. It is the mixture of fast time-scale processes (abrupt confinement bifurcations due to “spontaneous-like” ITB-events and global edge-core connection throughout RS zone at L-H-L transitions) described in the present paper and slow time scale processes (HPP and gradual variations of the confinement, strong linkage of current and pressure profiles [1] in RS plasmas).

The authors express their gratitude to Drs. T. Ozeki, R. Yoshino, T. Fukuda, S. Ide, S. Takeji for their continuous encouragements and fruitful discussion. They also thank JT-60 team for the fine collaboration. This work was carried out during SVN's stay at JAERI under JAERI Research Fellowship.

References

- [1] FUJITA, T., et al., Nucl. Fusion **39** (1999) 1627 and rep. EX4/1 at this conference.
- [2] KAMADA, Y., et al., Nucl. Fusion **39** (1999) 1680 and rep. OV1/1 at this conference.
- [3] FUJITA, T., IDE, H., KIMURA, S. et al., 16th IAEA Fusion Energy Conf. (Montreal, 1996), IAEA, Vienna (1997) vol. 1, p. 227.
- [4] NEUDATCHIN, S. V., TAKIZUKA, T., SHIRAI, H., FUJITA, T., ISEI, N., ISAYAMA, A., KOIDE, Y., KAMADA, Y., Plasma Phys. Control. Fusion **41** (1999) L39.
- [5] NEUDATCHIN, S. V., et al., Proc. 24th EPS Conf. on Control. Fus. and Plasma Phys., (Berchtesgaden, 1997), vol. 21A, (Geneva:EPS), part II, p. 497.
- [6] SHIRAI, H., KIKUCHI, M., TAKIZUKA, T., et al., Nucl. Fusion **39** (1999) 1713.
- [7] NEUDATCHIN, S. V., TAKIZUKA, T., SHIRAI, H., et al., “Analysis of internal transport barrier heat diffusivity from heat pulse propagation induced by ITB-event in JT-60U reverse shear plasmas”, submitted to Plasma Phys. Control. Fusion.
- [8] DNESTROVSKIJ, Yu. N., et al., Nucl. Fusion **39** (1999) 2089.
- [9] NEUDATCHIN, S. V., TAKIZUKA, T., SHIRAI, H., ISEI, N., KAMADA, Y., KOIDE, Y., SATO, M., AZUMI, M., Japan J. Appl. Phys. **35** (1996) 3595.
- [10] NEUDATCHIN, S. V., CORDEY, J. G., and MUIR, D. J., “The time behaviour of the electron conductivity during L-H and H-L transitions in JET” JET Rep. JET-P (93)-58 (1993)